PHYSICAL REVIEW D **92,** 063013 (2015)

Laser interferometer response to scalar massive gravitational waves

Arkadiusz Błaut
Institute of Theoretical Physics, University of Wrocław, Wrocław, Poland
(Received 31 March 2015; published 21 September 2015)

We analyze the response of the gravitational wave detector to a scalar massive plane gravitational wave. We give the compact form of the response and discuss its angular and frequency characteristics. The derivations are carried out in the conformal and the synchronous gauges, and the equivalence of the two approaches is shown. In a particular example of the massive Brans–Dicke theory, we show as well the equivalence of the two gauges on the level of the solution of the linearized field equation.

DOI: 10.1103/PhysRevD.92.063013 PACS numbers: 95.55.Ym, 04.80.Nn, 95.75.Pq, 97.60.Gb

I. INTRODUCTION

Alternatives to the general theory of relativity (GR) were present already in the early times of its birth and subsequent periods of its development, but they have been drawing particular attention in the last two decades. The early attempts (see Ref. [1] and references therein) aimed at founding a theoretical framework for the ongoing weak-field, low-energy experiments in the Earth and the Solar System gravitational environments, strong-field astrophysical observations like those of pulsars and compact binary systems, and then future gravitational wave detection experiments [2] exploring the dynamical, strong-field regime of gravity. The principal theoretical motivation for studying extensions of GR have been the unification of gravity with the rest of the Standard Model (SM) interactions [3] and the formulation of the consistent quantum theory of gravity—both issues still await fully satisfactory solutions. Nevertheless, the studies of high-energy unification models (string theory, supergravity, effective theories emerging from quantum gravity, brane-world models, extradimensional models, theories with noncommutative geometries, and theories based on deformed Lorentz symmetries) predict deviations from GR at some high-energy level and in a lower-energy limit lead to a number of competing effective theories. But can we expect modifications of GR at the low-energy scale as well? This cannot be excluded; although GR so far has passed safely most of the local weak-field and strong-field astrophysical tests, it is well known that it needs an additional hypothetical contribution known as a dark matter to explain the galactic and cluster scale observations of the rotation profiles [4,5]. Recently, the new motivations have come from cosmology: observations of the Supernovae Type Ia [6] and cosmic microwave background radiation anisotropies [7] revealed the accelerated expansion of the Universe favoring the Lambda cold dark matter (ΛCDM) model with another "dark" component dubbed dark energy. It is also well known that modified gravity can play a role in the early-time cosmology. The first inflationary scenario was proposed in the Starobinsky $f(R) = R + R^2/6M^2$ model [8]; the improvement of the chaotic inflation through the nonminimal coupling $\zeta\Phi^2 R$ of gravity and matter was proposed in Ref. [9]; and an interesting example of the unified picture of the gravity and SM particle physics was given in Ref. [10], where it was argued that the SM Higgs field H strongly nonminimally coupled to gravity, $\zeta H H^\dagger R$, $\zeta \gg 1$, can give rise to inflation. (For a review of modified gravity in cosmology, see, e.g., Ref. [11]). Furthermore, one expects that working ground-based gravitational wave detectors such as the Advanced Laser Interferometer Gravitational Observatory [12] or the planned next-generations ET [13] and space-based evolved Laser Interferometer Space Antenna (eLISA) [14] will give a unique opportunity to test GR and possibly to find some interesting observational challenges pointing to a new gravitational physics. In this respect, it is quite important to know the signals at the detector to discern between competing theories.

In this paper, we analyze the response of the gravitational wave interferometer to gravitational wave signals that arise in scalar-tensor (ST) theories (see, e.g., Ref. [15]). In those theories, gravitational interactions are mediated by a non-minimally coupled massless helicity 2 field and a scalar field. In the most studied example, the Brans–Dicke (BD) theory [16], the scalar field was massless, but recently the massive scalar fields have been investigated for a potential role they can play in the early- and late-time cosmology and in astrophysics [17–19]. It was also recognized that the Brans–Dicke theory with the BD parameter ω_{BD} equal to zero contains as a subclass the so-called extended theories of gravity with gravitational action defined by some function $f(R)$ of the scalar curvature [19,20]. In both those theories, matter fields are coupled minimally to the tensor field $g_{\mu\nu}$. Dynamics of the metric field, however, differs from the dynamics in GR due to the nontrivial interaction of the metric with the scalar field in the ST theories and due to the modified field equations in the case of extended theories. For the gravitational waves, this shows up as an additional, in general massive, spin-zero mode of the wave that potentially can be detected by interferometers.

Gravitational waves were also studied in other generalized theories. Recently, an exact plane wave solution was found in Ref. [21] for a class of Horndeski theory [22], which can be considered as a generalization of the scalar-tensor Brans–Dicke theory, and in Ref. [23] in the case of the nonlinear massive dRGT gravity model [24].

The nonrelativistic sector of gravitational interactions in these theories is also modified. For example, if the scalar field in massive BD theory satisfies the Klein–Gordon equation with the mass parameter m, one expects that the effective Newtonian gravitational potential in the near zone of a source will be modified by the Yukawa-type corrections, $\sim \exp(-mr)$. These corrections would manifest themselves as a deviation from Keppler's third law and can be investigated by observing the dynamics of the planets of the Solar System [25]. The uncertainty of those measurements can be interpreted as providing the upper bounds on the mass parameter. The strongest upper bound, $m < 4.4 \times 10^{-22}$ eV, comes from the observations of Mars [26]. But whatever the Solar System bounds might be, one must take notice that in theories predicting massive scalar waves the mass parameter may have a dynamical origin. For example, in massive ST theories, it is defined by the local minimum of some potential $V(\phi)$ which determines the dynamics of ϕ. However, one can also consider potentials having a number of local extrema which, depending on the external conditions and directly on the value of the scalar field, could lead to different dynamically generated masses. This would not be an unusual scenario, and in fact it is analogous to the SM Higgs mechanism for spontaneous mass generation. The desired nonperturbative effect in ST theory would be the *scalarization* phenomenon in neutron stars where nontrivial configurations of a large scalar field can appear [27]. Another example comes from Einstein–Aether theory, which predicts gravitational waves of different polarizations and different propagation speeds although all modes are massless; i.e., their frequencies are proportional to wave vectors [28]. These examples illustrate that the relativistic, strong-field domain may have quite distinctive features compared to those predicted or extrapolated from the nonrelativistic and low-energy ranges and show that the gravitational waves may be good probes in exploring this regime.

The response of the gravitational wave detectors to the scalar mode was investigated already in Refs. [29–32], and the detection capability together with astrophysical and cosmological application were presented in Refs. [31,33–35]. Here, we continue these efforts and further analyze the detector response. We present the compact form of the detector response for massive scalar perturbations that straightforwardly reveals the angular and frequency characteristics of the antenna in the whole frequency domain. The detector response is obtained by analyzing the motion of the emitter, detector, and laser light in the conformal gauge and synchronous gauge. Working in the synchronous gauge in which the free motion of test particles (thus, e.g., emitters, beam splitters of a freely falling gravitational wave detectors) can be easily computed is particularly convenient for space-based interferometers where the high-frequency domain of the detector response usually plays an important role. Furthermore, we show the equivalence of the two gauges by giving the explicit gauge transformation for the massive scalar wave solutions. This result is also generalized to theories in which a scalar field can have modified dispersion relations.

The paper is organized as follows. In Sec. II, we recount the massive Branse–Dicke theory. In Sec. III, we investigate the detector response in the conformal gauge, and in Sec. IV, we investigate the response in the synchronous gauge. In Sec. V, we give the angular and frequency characteristics of the one-arm one-way detector. In Appendix A, we recall the definitions of the scalar polarization tensors; in Appendix B, we derive the vacuum plane wave solution in the linearized massive Brans–Dicke theory, working directly in the synchronous gauge; in Appendix C, we show the equivalence of the two gauges by explicitly giving the gauge transformation.

Greek letters denote spacetime indices and take the values 0, 1, 2, 3; Latin letters i, j, k denote space indices and take the values 1, 2, 3; coordinates (x^0, x^1, x^2, x^3) are denoted also as (t, x, y, z); colon ":" denotes contraction of tensors..

II. MASSIVE BRANS–DICKE GRAVITY

In this section, we give a brief account of the theory in which the gravitational interaction is mediated by two fields, the standard metric tensor field and the massive scalar field. We rederive solutions of the linearized field equations for the general gravitational wave comprising two massless tensor modes and one massive scalar mode.

We recall that a class of massive scalar-tensor theories described by the action

$$S[g_{\mu\nu}, \phi, \psi_m] = S_g[g_{\mu\nu}, \phi] + S_m[g_{\mu\nu}, \psi_{\rm m}], \tag{2.1}$$

$$S_g[g_{\mu\nu}, \phi] = \frac{1}{16\pi} \int d^4x \sqrt{-g} \left[\phi R - \frac{\omega(\phi)}{\phi} \partial^\mu \phi \partial_\mu \phi + V(\phi) \right], \tag{2.2}$$

$$S_m[g_{\mu\nu}, \psi_{\rm m}] = \int d^4x \sqrt{-g} L_{\rm m}[\psi_{\rm m}, g_{\mu\nu}], \tag{2.3}$$

where $g_{\mu\nu}$ is a metric field, ϕ is a scalar field, and $\psi_{\rm m}$ denotes collection of matter fields, were introduced in Refs. [36] and [37]. Here, ω and V are two coupling functions, and R is the scalar curvature of the metric. The effects of the function ω on the dynamics of compact binaries have been extensively studied in Refs. [38–41] or in the cosmological context in Ref. [42]. The self-interaction potential V in turn can play a role of the cosmological constant and give rise to a mass term in the linearized theory.

In what follows, we consider the massive Brans–Dicke theory in which the coupling parameter ω is given by the constant Brans–Dicke parameter, $\omega(\phi) = \omega_{\rm BD}$. The field equations obtained by varying the action $S[g_{\mu\nu}, \phi]$ with respect to the metric $g_{\mu\nu}$ and the scalar field ϕ are given by [15]

$$\begin{aligned} R_{\mu\nu} - \frac{1}{2} g_{\mu\nu} R - \frac{V(\phi)}{\phi} &= \frac{8\pi T_{\mu\nu}}{\phi} + \frac{\omega_{\rm BD}}{\phi^2}\left(\phi_{,\mu}\phi_{,\mu} - \frac{1}{2} g_{\mu\nu}\phi_{,\alpha}\phi^{,\alpha}\right) + \frac{\phi_{,\mu\nu} - \Box_g \phi}{\phi}, \\ \Box_g \phi + \frac{\phi V'(\phi) - 2V(\phi)}{3 + 2\omega_{\rm BD}} &= \frac{8\pi T}{3 + 2\omega_{\rm BD}}, \end{aligned} \tag{2.4}$$

where $R_{\mu\nu}$ is the Ricci tensor, $\Box_g \equiv (-g)^{-1/2}\partial_\mu(-g)^{1/2} g^{\mu\nu}\partial_\nu$, $T^{\mu\nu} \equiv \frac{2}{\sqrt{-g}}\frac{\delta S}{\delta g_{\mu\nu}}$, $T \equiv g_{\mu\nu}T^{\mu\nu}$, and $V' \equiv \frac{dV}{d\phi}$. We consider small perturbations over the background configuration of the Minkowski metric $\eta_{\mu\nu}$ and a constant field $\phi(x) = \phi_0$,

$$\begin{aligned} g_{\mu\nu} &= \eta_{\mu\nu} + h_{\mu\nu}, \qquad \phi = \phi_0 + \delta\phi, \\ |h_{\mu\nu}| &\ll 1, \qquad |\delta\phi| \ll 1. \end{aligned} \tag{2.5}$$

To preserve the asymptotic flatness of solutions and to neglect higher-order self-interaction terms for the scalar field beside the mass term, we assume [18] $V(\phi) = \frac{1}{2}V''(\phi_0)\delta\phi^2$. Substituting (2.5) into the field equations (2.4) and introducing the mass of the scalar field $m^2 \equiv -\frac{\phi_0}{3+2\omega_{\rm BD}}V''(\phi_0)$, one finds

$$R^{(1)}_{\mu\nu} - \frac{1}{2} g_{\mu\nu} R^{(1)} = -\Phi_{,\mu\nu} + \eta_{\mu\nu}\Box_\eta \Phi \tag{2.6}$$

$$\Box_\eta \Phi = m^2 \Phi, \tag{2.7}$$

where $\Box_\eta \equiv \eta^{\mu\nu}\partial_\mu\partial_\nu$, $\Phi \equiv -\frac{\delta\phi}{\phi_0}$ and we denote $R^{(1)}_{\mu\alpha\nu\beta}$, $R^{(1)}_{\mu\nu}$, and $R^{(1)}$ as the linearizations of the Riemann tensor, Ricci tensor, and Ricci scalar to first order in $h_{\mu\nu}$, respectively (the explicit form of the $R^{(1)}_{\mu\alpha\nu\beta}$ is given in Ref. [43] and recalled in Appendix B).

One way to obtain the solutions of the linearized field equations (2.6), (2.7) (see, e.g., Ref. [30]) is to define

$$\theta_{\mu\nu} \equiv h_{\mu\nu} - \eta_{\mu\nu}\left(\frac{1}{2}h - \Phi\right), \qquad h = \eta^{\mu\nu}h_{\mu\nu} \tag{2.8}$$

and to use the gauge freedom $h_{\mu\nu} \to h'_{\mu\nu}$, $\phi \to \phi'$,

$$\begin{aligned} h'_{\mu\nu}(x) &= h_{\mu\nu}(x) - \zeta_{(\mu,\nu)}, \qquad |\zeta_\mu| \ll 1 \\ \phi'(x) &= \phi(x), \end{aligned} \tag{2.9}$$

with the gauge parameter ζ_μ satisfying

$$\Box_\eta \zeta_\mu = \theta_{\mu\nu}{}^{,\nu}, \tag{2.10}$$

to impose on $\theta_{\mu\nu}$ the Lorentz gauge condition (we omit primes in the transformed fields)

$$\theta^{\mu\nu}{}_{,\nu} = 0. \tag{2.11}$$

In this gauge, the field equations have the form of the wave and the Klein–Gordon equations in the flat spacetime,

$$\Box_\eta \theta_{\mu\nu} = 0, \tag{2.12}$$

$$\Box_\eta \Phi = m^2 \Phi, \tag{2.13}$$

describing the (superpositions) of the plane monochromatic waves

$$\begin{aligned} \theta_{\mu\nu} &= A_{\mu\nu}e^{-ik_\mu x^\mu}, \qquad k^\mu = (\omega, \mathbf{k}), \\ \omega &= |\mathbf{k}|, \qquad k_\mu A^{\mu\nu} = 0 \end{aligned} \tag{2.14}$$

$$\Phi = Ae^{-il_\mu x^\mu}, \qquad l^\mu = (\omega, \mathbf{l}), \qquad \omega = \sqrt{\mathbf{l}^2 + m^2}, \tag{2.15}$$

which can be written as

$$\theta_{\mu\nu} = A_{\mu\nu}e^{i\omega(t - \boldsymbol{\Omega}\cdot\mathbf{x})}, \qquad \boldsymbol{\Omega} = \mathbf{k}/|\mathbf{k}| \tag{2.16}$$

$$\Phi = Ae^{i\omega(t - \frac{\boldsymbol{\Omega}\cdot\mathbf{x}}{\mathrm{v}(\omega)})}, \qquad \boldsymbol{\Omega} = \mathbf{l}/|\mathbf{l}|, \tag{2.17}$$

where Ω's are unit vectors along the wave propagation and v is the ω-dependent phase velocity, $\mathrm{v}(\omega) = \frac{|\omega|}{\sqrt{\omega^2 - m^2}}$, of the scalar field. (The phase velocity diverges when ω tends to m. This is because the wavelength $\lambda = 2\pi/\sqrt{\omega^2 - m^2}$ grows then to infinity; in the limit $\omega = m$, the solutions of Eqs. (2.16) and (2.17) are therefore proportional to space-independent oscillations e^{imt}.) At this step, we have $h_{\mu\nu} = \theta_{\mu\nu} - \eta_{\mu\nu}(\frac{1}{2}\theta - \Phi)$, where $\theta = \eta^{\mu\nu}\theta_{\mu\nu}$ but the Lorentz condition (2.11) is preserved under the supplementary gauge transformation (2.9) with ζ_μ satisfying

$$\Box_\eta \zeta_\mu = 0, \tag{2.18}$$

$$\zeta^\mu{}_{,\mu} = -\frac{1}{2}\theta, \tag{2.19}$$

rendering the trace of $\theta_{\mu\nu}$ equal to zero and giving $h_{\mu\nu} = \theta_{\mu\nu} + \Phi\eta_{\mu\nu}$. The residual gauge freedom

$$\Box_\eta \zeta_\mu = 0, \tag{2.20}$$

$$\zeta^\mu{}_{,\mu} = 0 \tag{2.21}$$

is exactly the same as the gauge freedom that is left after specifying the Lorentz condition and imposing tracelessness on the metric perturbation in GR and can be used to transform $\theta_{\mu\nu}$ to the transverse-traceless (TT) form [43]. We call the resulting gauge the *conformal gauge* since it allows us to represent an arbitrary gravitational wave in the theory as a sum,

$$h_{\mu\nu}(t,\mathbf{x}) = A_{\mu\nu}(t,\mathbf{x}) + \Phi(t,\mathbf{x})\eta_{\mu\nu}, \tag{2.22}$$

of the TT wave $A_{\mu\nu}$ satisfying $A_{\mu 0} = 0$, $A^{ij}{}_{,j} = 0$, $A^i{}_i = 0$, and the scalar wave conformal to the Minkowski metric, $\Phi(t,\mathbf{x})\eta_{\mu\nu}$. For the plane wave propagating in the $-z$ direction, Eq. (2.22) simplifies to

$$h_{\mu\nu}(t,z) = A^+(t+z)\epsilon^+_{\mu\nu} + A^\times(t+z)\epsilon^\times_{\mu\nu} + \Phi(t,z)\epsilon^s_{\mu\nu}, \tag{2.23}$$

with the polarization tensors

$$\epsilon^s = \begin{pmatrix} -1 & 0 & 0 & 0 \\ 0 & 1 & 0 & 0 \\ 0 & 0 & 1 & 0 \\ 0 & 0 & 0 & 1 \end{pmatrix},$$
$$\epsilon^+ = \begin{pmatrix} 0 & 0 & 0 & 0 \\ 0 & 1 & 0 & 0 \\ 0 & 0 & -1 & 0 \\ 0 & 0 & 0 & 0 \end{pmatrix},$$
$$\epsilon^\times = \begin{pmatrix} 0 & 0 & 0 & 0 \\ 0 & 0 & 1 & 0 \\ 0 & 1 & 0 & 0 \\ 0 & 0 & 0 & 0 \end{pmatrix}. \tag{2.24}$$

In Appendix B, we derive the solutions to the linearized vacuum field equations (2.6), (2.7) directly in the gauge $h_{\mu 0} = 0$.

III. DETECTOR RESPONSE IN THE CONFORMAL GAUGE

In this section, we investigate the motion of a free test mass in the background field of the plane, massive scalar gravitational wave in the conformal gauge. The result will be next used in deriving the response of the laser interferometer in this gauge; here, we make use of the derivation given in Refs. [29] and [31] for the massless scalar field.

To this end, we first consider an arbitrary conformal wave moving in the direction $-z$ with the velocity v, $\mathrm{h}_s(t,z) = h_s(t+z/\mathrm{v})$ [so, e.g., it can be one of a Fourier modes of the Eq. (2.17)], in which case the background geometry has the form

$$ds^2 = \left[1 + h_s\left(t + \frac{z}{\mathrm{v}}\right)\right]\eta_{\mu\nu}dx^\mu dx^\nu. \tag{3.1}$$

The free motion of a test body can be obtained from the Lagrangian

$$L(\mathbf{x},\dot{\mathbf{x}}) = \frac{1}{2}\left[1 + h_s\left(t + \frac{z}{\mathrm{v}}\right)\right](-\dot{t}^2 + \dot{x}^2 + \dot{y}^2 + \dot{z}^2),$$

where the dot stands for the proper time derivative, $\dot{x}^\mu(\tau) \equiv \frac{dx^\mu(\tau)}{d\tau}$. The equations of motion read

$$\frac{d}{d\tau}[(1+h_s)\dot{t}] = -\frac{1}{2}\mathrm{h}_{s,t}(-\dot{t}^2 + \dot{x}^2 + \dot{y}^2 + \dot{z}^2) \tag{3.2}$$

$$\frac{d}{d\tau}[(1+h_s)\dot{x}^i] = \frac{1}{2}\mathrm{h}_{s,i}(-\dot{t}^2 + \dot{x}^2 + \dot{y}^2 + \dot{z}^2), \quad i = 1,2,3. \tag{3.3}$$

We assume that in the absence of gravitational wave the test body was at rest with respect to the coordinates, and hence we seek for the leading-order solution having the form $\dot{t} = 1 + A_t h$, $\dot{x}^i = A_i h$. From Eqs. (3.3), it follows that, as a first step, we can specify $A_x = A_y = 0$. Using the (leading-order) identities $\mathrm{h}_{s,t} = \dot{h}_s$ and $\mathrm{h}_{s,z} = \dot{h}_s/\mathrm{v}$ from Eqs. (3.2) and (3.3), it then follows that $A_t = -\frac{1}{2}$, $A_z = -\frac{1}{2\mathrm{v}}$, and we get

$$x(t) = x_0 \tag{3.4}$$

$$y(t) = y_0 \tag{3.5}$$

$$z(t) = z_0 - \frac{1}{2\mathrm{v}}\int_\infty^t h_s[t' + z(t')/\mathrm{v}]dt' = z_0 - \frac{1}{2\mathrm{v}}\int_\infty^{t+\frac{z_0}{\mathrm{v}}} h_s(v)dv \tag{3.6}$$

$$\tau(t) = t + \frac{1}{2}\int_\infty^{t+\frac{z_0}{\mathrm{v}}} h_s(v)dv, \tag{3.7}$$

where $v(t') = t' + z(t')/\mathrm{v}$ and x_0, y_0, z_0 are the initial positions set at $t \to -\infty$. To have the motion of the test particle in the case of the plane wave propagating along the unit vector $\Omega = (-\cos\phi\sin\theta, -\sin\phi\sin\theta, -\cos\theta)$, one rotates the frame,

$$\begin{pmatrix} x_{\text{new}} \\ y_{\text{new}} \\ z_{\text{new}} \end{pmatrix} = \begin{pmatrix} \cos\theta\cos\phi & -\sin\phi & \sin\theta\cos\phi \\ \cos\theta\sin\phi & \cos\phi & \sin\theta\sin\phi \\ -\sin\theta & 0 & \cos\theta \end{pmatrix} \begin{pmatrix} x \\ y \\ z \end{pmatrix}, \tag{3.8}$$

to get in the new coordinates (we omit the subindex new),

$$\mathbf{x}(t) = \mathbf{x}_0 + \frac{\Omega}{2\mathrm{v}} \int_{-\infty}^{t-\frac{\Omega\cdot\mathbf{x}_0}{\mathrm{v}}} h_s(v)dv \tag{3.9}$$

$$\tau(t) = t + \frac{1}{2} \int_{-\infty}^{t-\frac{\Omega\cdot\mathbf{x}_0}{\mathrm{v}}} h_s(v)dv, \tag{3.10}$$

with $\mathbf{x}_0 = (x_0, y_0, z_0)$ and $\Omega \cdot \mathbf{x}_0 = -x_0 \cos\phi \sin\theta - y_0 \sin\phi \sin\theta - z_0 \cos\theta$.

To obtain the detector response, we place the freely moving emitter and the detector initially at the points $\mathbf{x}_{E0}$ and $\mathbf{x}_{D0} = \mathbf{x}_{E0} + L\mathbf{n}_{ED}$, respectively, where $\mathbf{n}_{ED}$ is the unit vector from the emitter to the detector and L is the length of the detector arm both defined with respect to the three-dimensional Euclidean metric δ_{ij}. We assume that clocks that measure the proper times along the trajectories of the emitter and detector were synchronized in the absence of the wave. Then the time of flight of the light signal from E to D, $\Delta\tau_{ED}(t) \equiv \tau_D(t) - \tau_E[t - \delta t(t)]$, where t and $t - \delta t(t)$ are the coordinate times of the emission and the detection, respectively, is a coordinate-independent quantity; in fact, it enters the detector response of all the gravitational wave laser interferometers. Namely, if we compare a laser signal $A_E = A_L e^{i\omega_L \tau_E}$ with angular frequency ω_L sent from the emitter to the detector with the identical template laser signal $A_D = A_L e^{i\omega_L \tau_D}$ at the detector, the change in the phase will be proportional to $\Delta\tau_{ED}$:

$$\begin{aligned} &A_D(\tau_D(t)) - A_E[\tau_E(t - \delta t(t))] \\ &\quad \simeq A_L i\omega_L [\tau_D(t) - \tau_E[t - \delta t(t)]]. \end{aligned} \tag{3.11}$$

In the background given by Eq. (3.1), light travels along the null lines of the Minkowski metric $\eta_{\mu\nu}$ thus to the leading order

$$\begin{aligned} \delta t(t) &= |\mathbf{x}_D(t) - \mathbf{x}_E(t-L)| \\ &= \left| \mathbf{x}_{D0} - \mathbf{x}_{E0} + \frac{\Omega}{2\mathrm{v}} \int_{t-L-\frac{\Omega\cdot\mathbf{x}_{E0}}{\mathrm{v}}}^{t-\frac{\Omega\cdot\mathbf{x}_{D0}}{\mathrm{v}}} h_s(v)dv \right| \\ &\simeq L + \frac{\Omega\cdot\mathbf{n}_{ED}}{2\mathrm{v}} \int_{t-L-\frac{\Omega\cdot\mathbf{x}_{E0}}{\mathrm{v}}}^{t-\frac{\Omega\cdot\mathbf{x}_{D0}}{\mathrm{v}}} h_s(v)dv \end{aligned}$$

and using (3.10)

$$\begin{aligned} \Delta\tau_{ED}(t) &\simeq t + \frac{1}{2} \int_{\infty}^{t-\frac{\Omega\cdot\mathbf{x}_{D0}}{\mathrm{v}}} h_s(v)dv \\ &\quad - \left[t - L - \frac{\Omega\cdot\mathbf{n}_{ED}}{2\mathrm{v}} \int_{t-L-\frac{\Omega\cdot\mathbf{x}_{E0}}{\mathrm{v}}}^{t-\frac{\Omega\cdot\mathbf{x}_{D0}}{\mathrm{v}}} h_s(v)dv \right. \\ &\quad \left. + \frac{1}{2} \int_{\infty}^{t-L-\frac{\Omega\cdot\mathbf{x}_{E0}}{\mathrm{v}}} h_s(v)dv \right] \\ &= L + \frac{1}{2}\left(1 + \frac{\Omega\cdot\mathbf{n}_{ED}}{\mathrm{v}}\right) \int_{t-L-\frac{\Omega\cdot\mathbf{x}_{E0}}{\mathrm{v}}}^{t-\frac{\Omega\cdot\mathbf{x}_{D0}}{\mathrm{v}}} h_s(v)dv. \end{aligned} \tag{3.12}$$

In Eq. (3.6), we have parametrized the constant phase surfaces v's with the coordinate time t' along the particle trajectory. Now, we change the parametrization and will use a parameter λ along the laser ray. To this end, we notice that the trajectory $[\mathrm{t}_0(\lambda), \mathbf{x}_0(\lambda)]$ of the laser ray from $\mathbf{x}_{E0}$ to $\mathbf{x}_{D0}$ [end points are needed only in the zeroth order in the argument of the integrand h_s of Eq. (3.12)] is given by

$$\mathrm{t}_0(\lambda) = \lambda, \qquad \mathbf{x}_0(\lambda) = \mathbf{x}_{D0} - \mathbf{n}_{ED}(t - \lambda); \tag{3.13}$$

thus, changing the variables, $v(\lambda) = \mathrm{t}_0(\lambda) - \Omega\cdot\mathbf{x}_0(\lambda)/\mathrm{v}$, one finds

$$\begin{aligned} \Delta\tau_{ED}(t) &= L + \frac{1 - (\frac{\Omega\cdot\mathbf{n}_{ED}}{\mathrm{v}})^2}{2} \int_{t-L}^{t} h_s[v(\lambda)]d\lambda \\ &= L + \frac{1 - (\Omega\cdot\mathbf{n}_{ED})^2 + (1 - \frac{1}{\mathrm{v}^2})(\Omega\cdot\mathbf{n}_{ED})^2}{2} \\ &\quad \times \int_{t-L}^{t} h_s[v(\lambda)]d\lambda \\ &= L + \frac{\mathbf{n}_{ED} \otimes \mathbf{n}_{ED} : [\boldsymbol{\epsilon}^{st} + (1 - \frac{1}{\mathrm{v}^2})\boldsymbol{\epsilon}^{sl}]}{2} \\ &\quad \times \int_{t-L}^{t} h_s[v(\lambda)]d\lambda, \end{aligned} \tag{3.14}$$

where the 3×3 matrices, $\boldsymbol{\epsilon}^{st}$ and $\boldsymbol{\epsilon}^{sl}$, are defined in Appendix A. They play the role of the two (spatial) polarization tensors of the scalar transversal and scalar longitudinal modes of which the components in the synchronous gauge and in the source frame read

$$\epsilon^{st} = \begin{pmatrix} 1 & 0 & 0 \\ 0 & 1 & 0 \\ 0 & 0 & 0 \end{pmatrix}, \qquad \epsilon^{sl} = \begin{pmatrix} 0 & 0 & 0 \\ 0 & 0 & 0 \\ 0 & 0 & 1 \end{pmatrix}. \tag{3.15}$$

IV. DETECTOR RESPONSE IN THE SYNCHRONOUS GAUGE

In the synchronous gauge, the metric is given by

$$\mathbf{g} = -dt^2 + (\delta_{ij} + \mathrm{h}_{ij})dx^i dx^j. \tag{4.1}$$

The condition $\mathrm{h}_{\mu 0} = 0$ implies that the motion of test bodies is trivial: one can assume that the emitter and detector stay at fixed coordinates, $x^i(t) = \text{const.}$, and the coordinate time t is equal to the proper times along their trajectories, $\tau_E(t) = \tau_D(t) = t$. The time of flight is then equal to the difference in the coordinate times of the detection and emission and is given by the integral

$$\Delta\tau_{ED}(t) = \mathrm{t}(\lambda_D) - \mathrm{t}(\lambda_E) = \int_{\gamma_{ED}} \sqrt{\mathrm{g}_{ij}[\mathrm{t}(\lambda), \mathbf{x}(\lambda)] \frac{d\mathrm{x}^i}{d\lambda}\frac{d\mathrm{x}^j}{d\lambda}} d\lambda, \tag{4.2}$$

where $[\mathrm{t}(\lambda), \gamma_{ED}(\lambda)] = [\mathrm{t}(\lambda), \mathbf{x}(\lambda)]$ parametrizes the null geodesic of the light ray from the emitter to the detector with the arrival time at the detector $\mathrm{t}(\lambda_D) = t$. In the synchronous coordinates, trajectories of photons in the perturbed background (4.1) differ in general from straight lines, but as was shown by Finn [44] (see also Refs. [45] and [46]), the integral on the right-hand side of Eq. (4.2) is unchanged when computed along the *unperturbed* trajectory

$$\mathrm{t}_0(\lambda) = \lambda, \qquad \mathbf{x}_0(\lambda) = \mathbf{x}_D - \mathbf{n}_{ED}(t - \lambda). \tag{4.3}$$

This gives to the leading order

$$\begin{aligned} \Delta\tau_{ED}(t) &= L + \frac{\mathbf{n}_{ED} \otimes \mathbf{n}_{ED}}{2} : \int_{t-L}^{t} \mathbf{h}[\mathrm{t}_0(\lambda), \mathbf{x}_0(\lambda)]d\lambda \\ &= L + \frac{\mathbf{n}_{ED} \otimes \mathbf{n}_{ED} : \boldsymbol{\epsilon}^p}{2} \int_{t-L}^{t} h_p[v(\lambda)]d\lambda, \end{aligned} \tag{4.4}$$

where in the last line of Eq. (4.4) we have specified the p-polarized plane wave having the (spatial) polarization tensor $\boldsymbol{\epsilon}^p$ propagating along the vector $\boldsymbol{\Omega}$ with the velocity v, $\mathbf{h}(t, \mathbf{x}) = \boldsymbol{\epsilon}^p h_p(t - \boldsymbol{\Omega} \cdot \mathbf{x}/\mathrm{v})$, and we have defined $v(\lambda) = \mathrm{t}_0(\lambda) - \boldsymbol{\Omega} \cdot \mathbf{x}_0(\lambda)/\mathrm{v}$.

Comparison of Eqs. (4.4) and (3.14) suggests that the scalar wave defined in the conformal gauge corresponds to a superposition of scalar transversal and scalar longitudinal waves defined in the synchronous gauge (and in the frame in which the wave propagates in the $-z$ direction) as

$$ds^2 = -dt^2 + h_{st}\left(t + \frac{z}{\mathrm{v}}\right)(dx^2 + dy^2) + h_{sl}\left(t + \frac{z}{\mathrm{v}}\right)dz^2, \tag{4.5}$$

with

$$h_{st} = h_s, \qquad h_{sl} = \left(1 - \frac{1}{\mathrm{v}^2}\right)h_s. \tag{4.6}$$

This is indeed the case, and in Appendix C, we give the gauge transformation that connects both gauges. There, it is shown that a more general result holds: given a scalar mode $h_s(t, z)$ that in the conformal gauge satisfies the field equation $\partial_t^2 h_s = F[\partial_z]h_s$, the corresponding synchronous gauge wave is given by

$$\mathbf{h}(t, z) = \mathrm{diag}\left(0, h_s(t, z), h_s(t, z), \frac{F[\partial_z] - \partial_z^2}{F[\partial_z]} h_s(t, z)\right). \tag{4.7}$$

Beside the massive Brans–Dicke and $f(R)$ theories, this result includes also theories with a modified dispersion relation [47] that can arise, e.g., as the effective level of some approaches to quantum gravity or in Lorentz-symmetry violating theories [48–50]. We note here that usually the effects of modification of the dispersion relations are considered to be suppressed by the Planck scale, but Refs. [51] and [52] indicated the possibility of their enhancement when the renormalization is taken into account in Lorentz symmetry breaking models.

V. SENSITIVITY OF ONE-ARM INTERFEROMETER

Integration of the right-hand side Eq. (4.4) for the scalar monochromatic p-polarized wave $\mathrm{h}(t.\mathbf{x}) = h_p^0 e^{i\omega(t - \frac{\boldsymbol{\Omega}\cdot\mathbf{x}}{\mathrm{v}})}$ ($p = sl, st$) leads to the following result for the time-dependent part of the time of flight:

$$s_{ED}(t) \equiv \frac{\Delta\tau_{ED}(t)}{T} = F^p(\mathbf{n}_{ED})\mathcal{T}(x; c_{ED})\mathrm{h}(t, \mathbf{x}_D), \tag{5.1}$$

where $c_{ED} \equiv \frac{\boldsymbol{\Omega}\cdot\mathbf{n}_{ED}}{\mathrm{v}}$, $x \equiv L\omega$, $F^p(\mathbf{n}_{ED}) \coloneqq \frac{1}{2}\mathbf{n}_{ED} \otimes \mathbf{n}_{ED} : \boldsymbol{\epsilon}^p$ is the (one-arm) antenna pattern function, and $\mathcal{T}(x; c_{ED}) \equiv \mathrm{sinc}[\frac{x(1-c_{ED})}{2}]e^{-i\frac{x(1-c_{ED})}{2}}$ is the frequency response of the (one-arm and one-way) detector.

It was already observed in Ref. [53] that the frequency-independent maximum of the frequency transfer function, $\mathcal{T} = 1$, is achieved when the wave passes through the arm at the particular angle $\boldsymbol{\Omega} \cdot \mathbf{n}_{ED} = \cos\vartheta = \mathrm{v}$, and this is only possible when $\mathrm{v} \leq 1$; this is illustrated in Fig. 1(a). To see

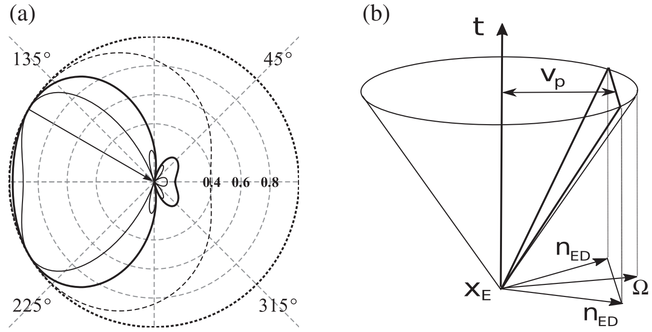

FIG. 1. Left: plane section of the frequency transfer function $|\mathcal{T}|$. The arm $\mathbf{n}_{ED}$ of the detector is inclined at 0°, $\mathrm{v} = \mathbf{\Omega} \cdot \mathbf{n}_{ED} = \cos\frac{\pi}{6}$; the arrow represents one of the directions $\Omega_{\max}$ of the maximal sensitivity. The normalized frequencies $x = \omega L$ equal zero (dotted), 2 (dashed), 5 (thick), and 10 (thin). Right: section of the null cone and the hypersurface of the constant phase passing through the emitter.

the geometrical picture behind that angle, we notice first that it is zero when $\mathrm{v} = 1$. In this case, as remarked in Refs. [46] and [45], the one-arm frequency transfer function $\mathcal{T}$ does not depend on frequency. This, together with nonvanishing antenna pattern function along the detector's arm for the scalar longitudinal mode, leads to the preferable detection feasibility at high frequencies for that mode. The reason for this is simple: the spacetime trajectory of the light ray lies on the three-dimensional hypersurface of the constant phase of the passing plane gravitational wave, and therefore photons perceive it as a constant field. The same is true for $\mathrm{v} < 1$, but in this case, planes of the constant phases of the gravitational wave are no longer tangent to null cones of the light rays. In the case of $\mathrm{v} < 1$, the light cone formed by light rays emitted from $\mathbf{x}_E$ and the plane of the constant phase passing through $\mathbf{x}_E$ intersect, and the null lines of the intersection determine a set of null trajectories that satisfy $\mathbf{\Omega} \cdot \mathbf{n}_{ED} = \mathrm{v}$; see Fig. 1(b). For $\mathrm{v} > 1$, light cones and planes of the constant phases do not intersect, and the effect does not arise. Interestingly, for $\mathrm{v} < 1$, the direction of the maximum has nonvanishing components parallel and orthogonal to $\mathbf{n}_{ED}$, and thus one expects that all polarization modes of gravitational waves, transversal and longitudinal, will share the property of having frequency-independent one-arm response functions, $F^p(\mathbf{n}_{ED})\mathcal{T}(x; c_{ED})$, in the directions determined by $\mathbf{\Omega} \cdot \mathbf{n}_{ED} = \mathrm{v}$ [see Figs. 2(a) and 2(b)]. In fact, this feature for the + and × tensorial modes was explored in Ref. [53] and used in putting the limits on the speed of gravitational waves from pulsar timing and providing a bound on the graviton mass $m_g \leq 8.5 \times 10^{-24}$ eV. Here, however, we restrict ourselves from the beginning to the theories in which the standard + and × modes travel with the speed of light unlike the scalar modes of which the amplitudes as shown in the previous chapter are related. Thus, the detector response for the scalar wave having in the conformal gauge the form $[(1 + \mathrm{h}_s(t, \mathbf{x})]\eta_{\mu\nu}$ with the amplitude $\mathrm{h}_s(t, \mathbf{x}) = h_s^0 e^{i\omega(t - \mathbf{\Omega}\cdot\mathbf{x}/\mathrm{v})}$ is given by the Eq. (5.1) with the antenna pattern function that reads

$$F^s(\mathbf{n}_{ED}) = F^{st}(\mathbf{n}_{ED}) + \left(1 - \frac{1}{\mathrm{v}^2}\right) F^{sl}(\mathbf{n}_{ED})$$
$$= \frac{1}{2} - \frac{1}{\mathrm{v}^2} F^{sl}(\mathbf{n}_{ED}) = \frac{\mathrm{v}^2 - (\mathbf{\Omega} \cdot \mathbf{n}_{ED})^2}{2\mathrm{v}^2}, \quad (5.2)$$

if we use $F^{st} + F^{sl} = \frac{1}{2}$, $F^{sl} = \frac{1}{2}(\mathbf{\Omega} \cdot \mathbf{n}_{ED})^2$. We notice that the antenna pattern function F^s must preserve the property of frequency-independence for the detector response for the wave coming from the direction determined by $\mathbf{\Omega} \cdot \mathbf{n}_{ED} = \mathrm{v}$ since both antenna patterns F^{st} and F^{sl} do. But interestingly, for the particular combination of the scalar modes which is motivated on the theoretical grounds by the massive scalar-tensor theories, the net sensitivity is null for $\mathbf{\Omega} \cdot \mathbf{n}_{ED} = \mathrm{v}$, [see Eq. (5.2) and Fig. 2(c)].

Similarly, one can obtain the detector response for the scalar wave that in the conformal gauge has the form

$$\mathrm{h}_s(t, \mathbf{x}) = h_s^0 \boldsymbol{\epsilon}^p \cos\left[\omega\left(t - \frac{\mathbf{\Omega} \cdot \mathbf{x}}{\mathrm{v}}\right) + \phi_0\right]; \quad (5.3)$$

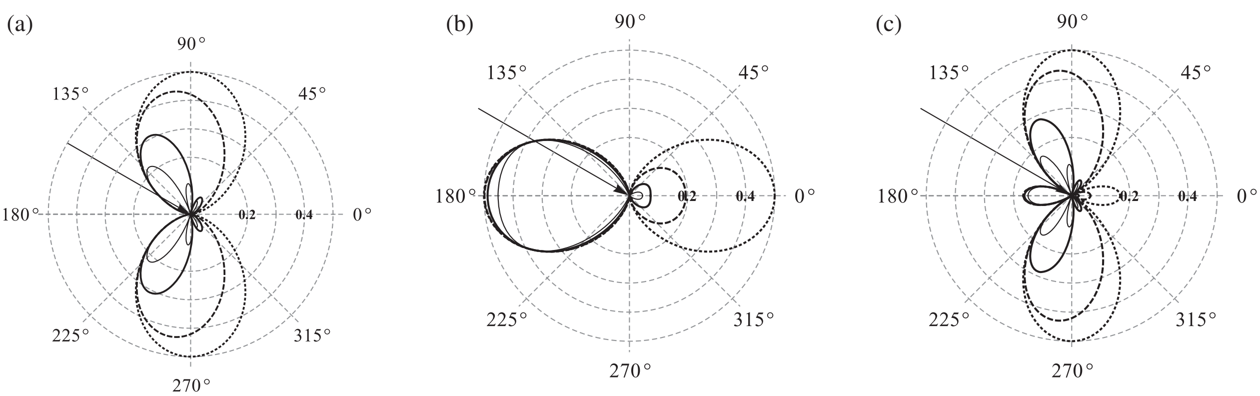

FIG. 2. Planar sections of the detector response $|F^p(\mathbf{n}_{ED})\mathcal{T}(x; c_{ED})|$ for the st (a), sl (b), and s (c) modes; notation and parameters as in Fig. 1. In cases a, b, c, responses for the signal coming from 150° are frequency independent; for c, it is zero.

it is given by [the real part of Eq. (5.1)

$$s_{ED}(t) = \mathrm{sinc}\left[\frac{x(1-c_{ED})}{2}\right] F^s(\mathbf{n}_{ED}) h_s^0 \times \cos\left[\omega\left(t - \frac{\Omega\cdot\mathbf{x}_E}{\mathrm{v}}\right) - \frac{x}{2}(1+c_{ED}) + \phi_0\right]. \tag{5.4}$$

We see that, due to the relation (4.6) between the scalar transversal and longitudinal modes, the initial phase ϕ_0 of the h^{st} and h^{sl} signals is the same. From the one-arm response, one can construct in a standard way other responses; e.g., the Michelson interferometer based on $\mathbf{n}_{ED_1}$ and $\mathbf{n}_{ED_2}$ is defined as

$$M(t) = s_{ED_1}(t-L) + s_{D_1E}(t) - s_{ED_2}(t-L) - s_{D_2E}(t). \tag{5.5}$$

Furthermore, we see that the long-wavelength (LW) limit defined as the leading x term of the response (5.4) is given by

$$s_{ED}^{\mathrm{LW}}(t) = F^s(\mathbf{n}_{ED}) h_s^0 \cos\left[\omega(t - \frac{\Omega\cdot\mathbf{x}_E}{\mathrm{v}}) + \phi_0\right], \tag{5.6}$$

so the corresponding Michelson interferometer M^{LW} will not discern h^s, h^{st}, and h^{sl} signals whatever the orientation of the two arms $\mathbf{n}_{ED_1}$ and $\mathbf{n}_{ED_2}$ is [note that the same is true for some other responses, e.g., the Sagnac interferometer $S(t) = s_{ED_1}(t-2L) + s_{D_1D_2}(t-L) + s_{D_2E}(t) - s_{ED_2}(t-2L) - s_{D_2D_1}(t-L) - s_{D_1E}(t)$]. However, beyond the LW limit, the responses of the Michelson interferometers M are different due to the orientation-dependent higher-frequency terms which potentially enable us to discriminate between the modes. On the other hand, the difference between the $\mathrm{v}=1$ and $\mathrm{v}\neq 1$ cases shows up already in the LW limit, for instance, in the massive Brans–Dicke theory as the corrections $\sim\Omega\cdot\mathbf{x}_E(\frac{m}{\omega})^2$ in the signal's phase.

VI. SUMMARY

The analysis of the response of the laser interferometer to passing gravitational waves is a starting point in the gravitational waves detection experiments. Especially at the present moment of awaiting the first detection by the advanced detectors, there is a good opportunity to routinely confront GR with the alternative theories testing gravity in the new dynamical, relativistic regime [54]. The theoretical framework for the classification of waves in alternative theories was given in Ref. [2] under the assumption of the minimal coupling of gravity to matter fields and with the restriction that the waves must travel at exactly the speed of light. The present paper deals with theories where the former assumption is fulfilled but the later restriction is relaxed. The detectability of gravitational wave signals in the massless scalar-tensor theory of Brans and Dicke where both modes, scalar and tensor, move with the speed of light was studied in Ref. [55] for inspiralling compact binaries. In Ref. [29], the detectability of massless scalar waves was investigated in the case of gravitational collapse, and the analysis of the detector response for those modes was also given. In this context, finding the detection methods to discern between the scalar and tensor waves and thorough analysis of the signals in the detector was desirable. With this aim, the rigorous examination of the frequency response and the antenna sensitivity pattern for the massless scalar waves was performed in Ref. [31] in the whole frequency domain; in Ref. [30], the detector response was analyzed in the conformal and in the synchronous gauges in the long wavelength limit, and the equivalence of the two approaches was demonstrated.

In the paper, we studied these basic issues in the case of the massive scalar wave. These kinds of perturbations can arise in a number of alternative theories; in particular, they can be realized in the massive Branse–Dicke theory or in a class of the $f(R)$ extended theories of gravity [33,56]. The detector response for this case was studied in Ref. [30] in the long wavelength limit and in Ref. [33] for the full frequency spectrum. Here, we carry out the analysis of the response of the laser interferometer to the scalar wave in the conformal gauge and in the synchronous gauge for all frequencies, and we show the equivalence of the two approaches. We show as well the equivalence of these two gauges on the level of the solutions of the linearized field equations of the massive Brans–Dicke theory. We present basic angular and frequency characteristics of the gravitational wave antenna. The response of the detector written in the synchronous gauge is particularly useful since in these coordinates the free motion of test bodies (like the beam splitter, mirrors, etc.) is simple. Thus, although the response was explicitly given for the static interferometer, the motion of the detector can straightforwardly be taken into account. This analysis can be applied to currently working Earth-based detectors and, in particular, to the future, next-generation experiments like the Einstein telescope or space-based missions like eLISA where it may be also essential to go beyond the long-wavelength approximation of the interferometer response, which is usually assumed when working in the local Lorentz frame.

ACKNOWLEDGMENTS

The work was supported in part by the National Science Centre Grants No. UMO-2013/01/ASPERA/ST9/00001 and No. UMO-2014/14/M/ST9/00707.

APPENDIX A: SCALAR POLARIZATION MODES

Let the orthonormal basis $\{\mathbf{e}_x, \mathbf{e}_y, \mathbf{e}_z \equiv \Omega\}$ represents the source frame and $\mathbf{n}$ be the unit vector along the detector arm; then,

$$\boldsymbol{\epsilon}^{sl} = \mathbf{e}_z \otimes \mathbf{e}_z = \Omega \otimes \Omega$$
$$\boldsymbol{\epsilon}^{st} = \mathbf{e}_x \otimes \mathbf{e}_x + \mathbf{e}_y \otimes \mathbf{e}_y, \tag{A1}$$

and thus

$$\mathbf{n} \otimes \mathbf{n}:\ \boldsymbol{\epsilon}^{sl} = (\mathbf{n} \cdot \Omega)^2$$
$$\mathbf{n} \otimes \mathbf{n}:\ \boldsymbol{\epsilon}^{st} = (\mathbf{n} \cdot \mathbf{e}_x)^2 + (\mathbf{n} \cdot \mathbf{e}_y)^2 = 1 - (\mathbf{n} \cdot \Omega)^2. \tag{A2}$$

We can now identify arbitrary Cartesian coordinates having $\{\mathbf{e}_x, \mathbf{e}_y, \mathbf{e}_z \equiv \Omega\}$ as an orthonormal basis with the spatial part of our synchronous coordinate system. We can aslo relate vectors and covectors in the canonical way: $\Omega_i = \Omega^j \delta_{ij} = \Omega^i$. Therefore, in arbitrary synchronous coordinates, the spatial tensors $\boldsymbol{\epsilon}^{st}$, $\boldsymbol{\epsilon}^{sl}$ can be written as

$$\boldsymbol{\epsilon}^{sl} = \Omega_i \Omega_j dx^i dx^j$$
$$\boldsymbol{\epsilon}^{st} = (\delta_{ij} - \Omega_i \Omega_j) dx^i dx^j. \tag{A3}$$

APPENDIX B: GRAVITATIONAL WAVES IN THE MASSIVE BRANS–DICKE THEORY IN THE SYNCHRONOUS GAUGE

In this Appendix, we obtain the solution of the linearized field equations (2.6), (2.7) in the gauge $h_{\mu 0} = 0$. To this end, we recall the explicit form of $R^{(1)}_{\mu\alpha\nu\beta}$ [43]:

$$R^{(1)}_{\mu\alpha\nu\beta} = \frac{1}{2}[h_{\mu\beta,\nu\alpha} + h_{\nu\alpha,\mu\beta} - h_{\mu\nu,\alpha\beta} - h_{\alpha\beta,\mu\nu}]. \tag{B1}$$

Now, we choose the gauge $h_{\mu 0} = 0$, and we assume the plane wave solutions $h_{ij}(t, z)$, $\Phi(t, z)$ for a wave propagating along the z direction; taking the spatial trace of the field Eqs. (2.6) and using Eq. (2.7), we obtain

$$-\Box_2 h_{11} - \Box_2 h_{22} + h_{33,tt} + 3m^2\Phi = 0, \quad \text{where } \Box_2 \equiv -\partial_t^2 + \partial_z^2. \tag{B2}$$

Substituting $h_{33,tt}$ obtained in Eq. (B2) to "11" and "22" components of Eqs. (2.6), one gets

$$\Box_2 h_{11} = m^2\Phi \tag{B3}$$

$$\Box_2 h_{22} = m^2\Phi, \tag{B4}$$

with the solutions $h_{11} = \Phi + h^0_{11}$ and $h_{22} = \Phi + h^0_{22}$, where h^0_{11} and h^0_{22} solve the homogeneous wave equation; in turn, the "00" component of (2.6),

$$-\frac{1}{2}h_{11,zz} - \frac{1}{2}h_{22,zz} + m^2\Phi + \Phi_{tt} = 0, \tag{B5}$$

imposes the trace-free condition for the homogeneous solutions, $h_+ \equiv h^0_{11} = -h^0_{22}$. From the "33" part of the system (2.6), using Eqs. (B2) and (B4), one obtains

$$h_{33,tt} = -m^2\Phi, \tag{B6}$$

whereas the "12" part gives

$$\Box_2 h_{12} = 0; \tag{B7}$$

the remaining equations (2.6) are identities or show that $h_{13} = h_{23} = 0$. Thus, the full set of modes consists of two standard massless helicity 2 states h_+, $h_\times \equiv h_{12}$, and two massive modes (but 1 degree of freedom), $h_{st} = \Phi$, $h_{sl} \equiv h_{33}$.

APPENDIX C: EQUIVALENCE OF THE CONFORMAL AND SYNCHRONOUS GAUGES

In this Appendix, we show the equivalence of the two gauges, the conformal gauge, Eq. (3.1), and the synchronous gauge, Eq. (4.5). Note that under three-dimensional rigid rotations in the conformal coordinates components of the gravitational wave tensor $h_s(t, \mathbf{x})\eta_{\mu\nu}$ transform as a set of four scalar fields, whereas in the synchronous gauge, the diagonal form of the tensor is not preserved, and thus one expects off-diagonal terms of the scalar modes as well which will mix with the transverse traceless modes. To simplify the calculations, we will treat here only the scalar modes; we will work in the frame in which the wave propagates in an arbitrary direction Ω;

First, we assume the gravitational wave of the form $h_s(t - \Omega \cdot \mathbf{x}/\mathrm{v})$. In this case, the transformation of coordinates

$$\mathbf{x} = \mathbf{x}' + \frac{1}{2}\mathbf{f}(t' - \Omega \cdot \mathbf{x}'/\mathrm{v}), \quad \mathbf{f}(t' - \Omega \cdot \mathbf{x}'/\mathrm{v}) = \frac{\Omega}{\mathrm{v}} \int_{-\infty}^{t' - \frac{\Omega \cdot \mathbf{x}'}{\mathrm{v}}} h_s(v) dv,$$
$$t = t' + \frac{1}{2}g(t' - \Omega \cdot \mathbf{x}'/\mathrm{v}), \quad g(t' - \Omega \cdot \mathbf{x}'/\mathrm{v}) = -\int_{-\infty}^{t' - \frac{\Omega \cdot \mathbf{x}'}{\mathrm{v}}} h_s(v) dv \tag{C1}$$

gives

$$
\begin{aligned}
d\mathbf{x} &= d\mathbf{x}' + \frac{\Omega}{2\mathrm{v}} h_s(t' - \Omega\cdot\mathbf{x}'/\mathrm{v})dt' \\
&\quad - \frac{\Omega}{2\mathrm{v}^2} h_s(t' - \Omega\cdot\mathbf{x}'/\mathrm{v})(\Omega\cdot d\mathbf{x}') \\
dt &= dt' - \frac{1}{2} h_s(t' - \Omega\cdot\mathbf{x}'/\mathrm{v})dt' \\
&\quad + \frac{1}{2\mathrm{v}} h_s(t' - \Omega\cdot\mathbf{x}'/\mathrm{v})(\Omega\cdot d\mathbf{x}'),
\end{aligned}
\tag{C2}
$$

which leads to

$$
\begin{aligned}
(1+h_s)\eta_{\mu\nu}dx^\mu dx^\nu &= \eta_{\mu\nu}dx'^\mu dx'^\nu + h_s(dx'^2 + dy'^2) \\
&\quad - \frac{\Omega_i\Omega_j}{\mathrm{v}^2} h_s dx'^i dx'^j \\
&= \eta_{\mu\nu}dx'^\mu dx'^\nu + \boldsymbol{\epsilon}^{st} h_s \\
&\quad + \left(1 - \frac{1}{\mathrm{v}^2}\right)\boldsymbol{\epsilon}^{sl} h_s,
\end{aligned}
\tag{C3}
$$

according to Eq. (A3).

For a superposition of monochromatic waves $e^{i\omega(t-\Omega\cdot\mathbf{x}/\mathrm{v})}$,

$$
\mathrm{h}_s(t,\mathbf{x}) = \int_m^\infty d\omega \int_{S^2} d\Omega e^{i\omega[t-\Omega\cdot\mathbf{x}/\mathrm{v}(\omega,\Omega)]}\chi(\omega,\Omega),
$$

where the form of a possibly orientation-dependent dispersion relation $\mathrm{v}(\omega,\Omega)$ is dictated by the field equations for h_s the generators $\mathbf{f}$, g of the gauge transformation, Eq. (C1), are given, respectively, by

$$
\begin{aligned}
&\frac{\Omega}{2\mathrm{v}}\int_m^\infty d\omega \int_{S^2} d\Omega \mathbf{f}[t' - \Omega\cdot\mathbf{x}'/\mathrm{v}(\omega,\Omega)], \\
&-\int_m^\infty d\omega \int_{S^2} d\Omega g[t' - \Omega\cdot\mathbf{x}'/\mathrm{v}(\omega,\Omega)],
\end{aligned}
$$

and then the scalar modes in the synchronous gauge read

$$
\begin{aligned}
&\int_m^\infty d\omega \int_{S^2} d\Omega\left[\boldsymbol{\epsilon}^{st}(\Omega) + \left(1 - \frac{1}{\mathrm{v}^2(\omega,\Omega)}\right)\boldsymbol{\epsilon}^{sl}(\Omega)\right] \\
&\quad\times e^{i\omega[t-\Omega\cdot\mathbf{x}/(\mathrm{v}\omega,\Omega)]}\chi(\omega,\Omega).
\end{aligned}
\tag{C4}
$$

As an example, let us consider the massive Brans–Dicke theory; in the conformal coordinates, we have

$$
\Box h_s = m^2 h_s, \qquad \mathrm{v}(\omega) = \frac{|\omega|}{\sqrt{\omega^2 - m^2}}, \qquad 1 - \frac{1}{\mathrm{v}^2(\omega)} = \frac{m^2}{\omega^2}.
$$

The gauge transformation (C1) for the plane wave propagating in the $-z$ direction, $h_s = \int_{-\infty}^\infty d\omega e^{i\omega(t+z/\mathrm{v})}\chi(\omega)$, with

$$
\begin{aligned}
\mathbf{f} &= \left(0, 0, \int_m^\infty d\omega \frac{i}{\omega\mathrm{v}} e^{i\omega(t+z/\mathrm{v})}\chi(\omega)\right), \\
g &= \int_m^\infty d\omega \frac{i}{\omega} e^{i\omega(t+z/\mathrm{v})}\chi(\omega)
\end{aligned}
\tag{C5}
$$

connects then

$$
\mathbf{h}(t,z) = \mathrm{diag}(-\mathrm{h}_s(t,z), \mathrm{h}_s(t,z), \mathrm{h}_s(t,z), \mathrm{h}_s(t,z))
\tag{C6}
$$

with

$$
\mathrm{h}'(t',z') = \mathrm{diag}\left(0, \mathrm{h}_s(t',z'), \mathrm{h}_s(t',z'), \frac{m^2}{-\partial_{z'}^2 + m^2}\mathrm{h}_s(t',z')\right).
\tag{C7}
$$

We see that the scalar mode has the same form as the solutions to the linearized field equations of the massive Brans–Dicke model obtained in Appendix B. Note that for $m = 0$ the generators of the gauge transformation given in Eq. (C1) or (C5) reduce to the transformation given in Ref. [30], Eqs. (B5) and (B6). We stress, however, that the result given here is more general: for any mode h_s that in the conformal gauge is constrained by the field equation $\partial_t^2 h_s = F[\partial_z]h_s$, the corresponding synchronous-gauge form of the wave (in the frame where the wave propagates along the z axis) reads

$$
\mathbf{h}(t,z) = \mathrm{diag}\left(0, \mathrm{h}_s(t,z), \mathrm{h}_s(t,z), \frac{F[\partial_z] - \partial_z^2}{F[\partial_z]}\mathrm{h}_s(t,z)\right).
\tag{C8}
$$

[1] C. M. Will, *Theory and Experiment in Gravitational Physics* (Cambridge University Press, Cambridge, England, 1993).
[2] D. M. Eardley, D. L. Lee, and A. P. Lightmann, Phys. Rev. D **8**, 3308 (1973).
[3] H. G. Goenner, Living Rev. Relativity **7**, 2 (2004).
[4] M. Milgrom, Astrophys. J. **270**, 365 (1983).
[5] J. D. Bekenstein, Phys. Rev. D **70**, 083509 (2004).
[6] A. G. Ries *et al.*, Astrophys. J. **607**, 665 (2004).
[7] Planck Collaboration, Astron. Astrophys. **A16**, 571 (2014).
[8] A. A. Starobinsky, Phys. Lett. **91B**, 99 (1980).
[9] R. Fakir and W. G. Unruh, Phys. Rev. D **41**, 1783 (1990).
[10] F. Bezrukov and M. Shaposhnikov, Phys. Lett. B **659**,703 (2008).
[11] T. Clifton, P. G. Ferreira, A. Padilla, and C. Skordis, Phys. Rep. **513**, 1 (2012).
[12] www.ligo.org.

[13] www.et-gw.eu.
[14] www.elisascience.org.
[15] Y. Fujii and K. Maeda, *The Scalar–Tensor Theory of Gravitation* (Cambridge University Press, Cambridge, England, 2003).
[16] C. Brans and R. Dicke, Phys. Rev. **124**, 925 (1961).
[17] N. Yunes, P. Pani, and V. Cardoso, Phys. Rev. D **85**, 102003 (2012).
[18] J. Alsing, E. Berti, C. M. Will, and H. Zaglauer, Phys. Rev. D **85**, 064041 (2012).
[19] A. De Felice and S. Tsujikawa, Living Rev. Relativity **13**, 3 (2010); S. Capozziello and M. De Laurentis, Phys. Rep. **509**, 167 (2011).
[20] T. P. Sotiriou and V. Faraoni, Rev. Mod. Phys. **82**, 451 (2010).
[21] E. Babichev, Phys. Rev. D **86**, 084037 (2012).
[22] G. W. Horndeski, Int. J. Theor. Phys. **10**, 363 (1974).
[23] M. Mohseni, Phys. Rev. D **84**, 064026 (2011).
[24] C. de Rham, G. Gabadadze, and A. J. Tolley, Phys. Rev. Lett. **106**, 231101 (2011).
[25] C. Talmadge, J.-P. Berthias, R. W. Hellings, and E. M. Standish, Phys. Rev. Lett. **61**, 1159 (1988).
[26] C. M. Will, Phys. Rev. D **57**, 2061 (1998).
[27] T. Damour and G. Esposito–Farese, Phys. Rev. Lett. **70**, 2220 (1993).
[28] T. Jacobson and D. Mattingly, Phys. Rev. D **70**, 024003 (2004).
[29] M. Shibata, K. Nakao, and T. Nakamura, Phys. Rev. D **50**, 7304 (1994).
[30] M. Maggiore and A. Nicolis, Phys. Rev. D **62**, 024004 (2000).
[31] K. I. Nakao, T. Harada, M. Shibata, S. Kawamura, and T. Nakamura, Phys. Rev. D **63**, 082001 (2001).
[32] C. Corda, J. Cosmol. Astropart. Phys., 04 (2007) 009.
[33] C. Capozziello, C. Corda, and M. De Laurentis, Phys. Lett. B **669**, 255 (2008).
[34] S. Bellucci, S. Capozziello, M. De Laurentis, and V. Faraoni, Phys. Rev. D **79**, 104004 (2009).
[35] N. Bonasia and M. Gasperini, Phys. Rev. D **71**, 104020 (2005).
[36] P. G. Bergmann, Int. J. Theor. Phys. **1**, 25 (1968).
[37] R. V. Wagoner, Phys. Rev. D **1**, 3209 (1970).
[38] C. M. Will and H. Zaglauer, Astrophys. J. **346**, 366 (1989).
[39] T. Damour and G. Esposito–Farése, Classical Quantum Gravity **9**, 2093 (1992).
[40] T. Damour and G. Esposito–Farése, Phys. Rev. D **53**, 5541 (1996).
[41] T. Damour and G. Esposito–Farése, Phys. Rev. D **54**, 1474 (1996).
[42] R. Nagata, T. Chiba, and N. Sugiyama, Phys. Rev. D **66**, 103510 (2002).
[43] C. Misner, K. Thorne, and J. A. Wheele, *Gravitation* (Freeman, New York, 1973).
[44] L. S. Finn, Phys. Rev. D **79**, 022002 (2009).
[45] A. Błaut, Phys. Rev. D **85**, 043005 (2012).
[46] M. Tinto and M. E. D. S. Alves, Phys. Rev. D **82**, 122003 (2010).
[47] S. Mirshekari, N. Yunes, and C. M. Will, Phys. Rev. D **85**, 024041 (2012).
[48] G. Amelino-Camelia, Nature (London) **418**, 34 (2002).
[49] P. Horava, J. High Energy Phys. 03 (2009) 020.
[50] T. Jacobson, *Proc. Sci.*, QG-PH (2007) 020.
[51] J. Collins, A. Perez, D. Sudarsky, L. Urrutia, and H. Vucetich, Phys. Rev. Lett. **93**, 191301 (2004).
[52] J. Collins, A. Perez, and D. Sudarsky, arXiv:hep-th/0603002.
[53] D. Baskaran, A. G. Polnarev, M. S. Pshirkov, and K. A. Postnov, Phys. Rev. D **78**, 044018 (2008); **78**, 089901(E) (2008).
[54] M. Isi, A. J. Weinstein, C. Mead, and M. Pitkin, Phys. Rev. D **91**, 082002 (2015).
[55] C. M. Will, Phys. Rev. D **50**, 6058 (1994).
[56] M. De Laurentis and S. Capozziello, Astropart. Phys. **35**, 257 (2011).